9. M. Liphardt *et al.*, *Science* **263**, 367 (1994).
10. K. Meerholz, B. L. Volodin, Sandalphon, B. Kippelen, N. Peyghambarian, *Nature* **371**, 497 (1994).
11. W. E. Moerner, S. M. Silence, F. Hache, G. C. Bjorklund, *J. Opt. Soc. Am. B* **11**, 320 (1994).
12. M. G. Kuzyk, J. E. Sohn, C. W. Dirk, *ibid.* **7**, 842 (1990).
13. J. W. Wu, *ibid.* **8**, 142 (1991).
14. D. J. Williams, in *Nonlinear Optical Properties of Organic Molecules and Crystals*, D. S. Chemla and J. Zyss, Eds. (Academic Press, Orlando, FL, 1987), vol. 1.
15. K. D. Singer, M. G. Kuzyk, J. E. Sohn, *J. Opt. Soc. Am. B* **4**, 968 (1987).
16. P. M. Lundquist *et al.*, *Science* **274**, 1182 (1996).
17. The value for Δn reported in table 2 of (*16*) for a sample with composition 2BNCM:PMMA:TNF 90:10:0.3 weight % is 10×10^{-3}. However, to be consistent with the four-wave mixing results presented in figure 1 of (*16*), this value should read 1.5×10^{-3}.
18. B. Kippelen, F. Meyers, N. Peyghambarian, S. R. Marder, *J. Am. Chem. Soc.* **119**, 4559 (1997).
19. H. Kogelnik, *Bell. Syst. Tech. J.* **48**, 2909 (1969). Kogelnik's coupled-wave theory for thick phase gratings predicts that the diffraction efficiency η is given by $\eta \propto \sin^2 \nu$ with $\nu = G\pi\Delta n d/\lambda$, where G is a geometrical factor that depends on the polarization of the beams and the experimental geometry, Δn is the dynamic range, d is the thickness of the grating, and λ is the wavelength of the light.
20. E. Hendrickx *et al.*, *Appl. Phys. Lett.* **71**, 1159 (1997).
21. B. Kippelen, Sandalphon, K. Meerholz, N. Peyghambarian, *ibid.* **68**, 1748 (1996).
22. J. L. Oudar and D. S. Chemla, *J. Chem. Phys.* **66**, 2664 (1977).
23. N. H. Abramson and K. G. Spears, *Appl. Opt.* **28**, 1834 (1989).
24. S. K. Gayen and R. R. Alfano, *Opt. Photonics News* **7**, 16 (1996).
25. D. D. Steele *et al.*, *Opt. Lett.*, in press.
26. S. C. W. Hyde *et al.*, *Ibid.* **20**, 1331 (1995).
27. Characterizing data: ^{1}H NMR ($CDCl_3$) δ 6.21 (s, 1H), 5.37 (s, 1H), 3.32–3.19 (m, 4H), 2.93–2.87 (m, 1H), 2.59–2.30 (m, 6H), 2.00 (m, 2H), 1.58–1.31 (m, 16H), 0.91 (t, J = 6.1 Hz, 6H). UV ($CHCl_3$) λ_{max} 496 (ε_{496} 113,500 M^{-1} cm^{-1}) nm; accurate fast atom bombardment mass spectrum (*m/z*) for M^+ $C_{25}H_{37}N_3$, calculated: 379.2987, found: 379.2979. Elemental analysis, calculated: C 79.11, H 9.82, N 11.07; found: C 78.81, H 10.01, N 10.97.
28. Supported by the U.S. Office of Naval Research (through the MURI Center CAMP), NSF, an international CNRS/NSF travel grant, the U.S. Air Force Office of Scientific Research, the U.S. Ballistic Missile Defense Organization, and a NATO travel grant. E.H. is a postdoctoral fellow of the Fund for Scientific Research–Flanders (Belgium). We thank A. Fort and M. Barzoukas from IPCMS (Strasbourg, France) for the dipole moment measurements, and P. M. Allemand for his help in the dielectric constant determination.

4 September 1997; accepted 10 November 1997

Electromechanical Properties of an Ultrathin Layer of Directionally Aligned Helical Polypeptides

T. Jaworek,* D. Neher, G. Wegner,† R. H. Wieringa, A. J. Schouten

The electromechanical properties of a monomolecular film of poly-γ-benzyl-L-glutamate (PBLG) 15 nanometers thick grafted at the carboxyl-terminal end to a flat aluminum surface were measured. The field-induced change in film thickness, dominated by a large inverse-piezoelectric effect, demonstrates that the "grafting-from" technique forces the chains into a parallel arrangement. The mechanical plate modulus of the film as determined by electrostriction agrees with the theoretical prediction for a single PBLG molecule along the chain axis. The experiments show that ultrathin polypeptide layers with large persistent polarization can be fabricated by the grafting approach.

One of the challenges of supramolecular chemistry is the manufacture of ultrathin layers with a perceptible and stable polar order. Such materials have potential in the construction of nanoscale piezo- and pyroelectric devices and for electrooptical applications. Techniques that have been used or suggested include the poling of initially nonpolar polymer films (*1*), the Langmuir-Blodgett (LB) assembly of polar monolayers (*2*), and, more recently, the defined growth of films of polar polymers by self-assembly (*3*) or grafting (*4*). In particular, the grafted films of polyglutamates have attracted interest for the fabrication of polar films (*4–10*). Poly-L-glutamates in the α-helical conformation are generally considered as prototype materials. The rodlike structure of the polar α-helix gives rise to some unique properties such as a high persistence length and large optical and mechanical anisotropy. In the helical conformation, the dipole moments of the individual repeat units along the chain add up to a large total dipole moment (*11*). Attempts have been made to orient polyglutamates by an electric field (*12*), and the net orientation was investigated by x-ray diffraction or second harmonic generation. However, as a consequence of the large dipole moment, the polar alignment of neighboring polypeptides helices is energetically unfavorable.

The "grafting-from" approach makes possible the directional alignment of the helical molecules (Fig. 1), as was first demonstrated by the work of Whitesell and Chang (*6*). These investigators first decorated the surface of a flat metal or metal oxide film with a layer of organic material exhibiting free amino groups by a self-assembly process and then started the polymerization of *N*-carboxyanhydrides of α-L-amino acids (NCAs) to obtain poly-L-amino acids. These amino acids are covalently attached at their COOH-terminal end to the surface and, depending on the type of amino acid used, grow directly in a helical conformation. Whitesell and Chang concluded that the chain orientation is mainly normal to the surface (*6*). However, to date, there is no conclusive evidence for proposed polar order in grafted polypeptide films.

We have measured the electromechanical properties of a grafted layer of poly-γ-benzyl-L-glutamate (PBLG) using a Nomarski optical interferometer (Fig. 2). Winkelhahn *et al.* have shown that this setup is capable of detecting periodic thickness changes with subpicometer resolution at modulation frequencies between 10 Hz and 100 kHz (*13*, *14*). The experimental data can yield the degree of polar order and the mechanical plate modulus of the ultrathin layer.

We constructed sandwich-type structures by growing a thin layer of PBLG on the surface of a glass substrate previously coated with thin aluminum strip electrodes (*15*). The self-assembled initiator layer was derived from triethoxy aminopropylsilane according to the procedure of Haller (*16*). This process generates a large surface density of amines on the substrate and prevents pinholes due to holes in the initiator layer (*17*). The surface graft polymerization initiated by the surface-anchored amino groups was carried out at 40°C in a 0.5 M solution of *N*-carboxyanhydride monomer in *N*,*N*-dimethylformamide for 2 days under nitrogen atmosphere. Further experimental details on the polymerization will be published elsewhere (*18*). The thickness of the grafted layer was 15 nm, as determined with a Tencor α-step profiler (*19*). The top aluminum strip electrodes were deposited with an orientation perpendicular to that of the bottom strips. In this way six independent

T. Jaworek, D. Neher, G. Wegner, Max-Planck-Institut für Polymerforschung, Ackermannweg 10, 55128 Mainz, Germany.
R. H. Wieringa and A. J. Schouten, Department of Polymer Chemistry, University of Groningen, Nijenborgh 4, 9747 AG Groningen, Netherlands.

*Present address: Tokyo Institute of Technology, Research Laboratory of Resources Utilization, 4259 Nagatsuta, Midori-ku, Yokohama, 226 Japan.
†To whom correspondence should be addressed. E-mail: wegner@mpip-mainz.mpg.de

capacitors with an area of 16 mm^2 were formed, of which two were functional.

A second PBLG film was grafted onto an aluminum-coated glass substrate under identical conditions and analyzed by infrared (IR) spectroscopy. The grafted polymer chains exist in the α-helical conformation, as demonstrated by the spectral positions of the amide I (1655 cm^{-1}) and amide II (1551 cm^{-1}) absorption bands (Fig. 3A). In the grazing-incidence IR (GIR) absorption spectrum only vibrations with transition dipole moments perpendicular to the substrate are observed. Because the transition dipole moment of the amide I vibration is directed almost parallel to the polymer backbone, LB films with PBLG helices oriented parallel to the substrate have rather weak amide I bands (Fig. 3B). In contrast, the PBLG grafted layer shows amide I and amide II bands of similar strength (*20*). This means that the helices are standing upright on the surface although they are presumably tilted significantly toward the substrate. This second sample was further characterized by x-ray photoelectron spectroscopy (XPS) experiments. The sample exhibited a uniform, substrate-free signal indicative of a homogeneous film with low pinhole density.

The electromechanical experiment measures the change in film thickness h as a function of the applied electric field E:

$$h(E) = h_0(1 + dE + aE^2 + ...) \quad (1)$$

where d is the inverse-piezoelectric coefficient, a is the electrostriction coefficient of the polymer layer, and h_0 is the film thickness without external bias. For an ac electric field with amplitude E_{AC} and frequency ω, the field-induced thickness change Δh as a function of time t is given by

$$\frac{\Delta h(E)}{h_0} = \frac{1}{2}aE_{AC}^2 + d(\omega)E_{AC}\cos(\omega t) + \frac{1}{2}a(2\omega)E_{AC}^2\cos(2\omega t) \quad (2)$$

with frequency components at 0ω, 1ω, and 2ω. In the experiment we separated the different contributions using frequency-selective lock-in detection.

We investigated the inverse-piezoelectric and electrostriction response of the grafted film for a range of frequencies of the film thickness modulation (Fig. 4 and Table 1). Both intact capacitors gave comparable results. Expressions for d and a are derived in (*13, 14, 21*):

$$a(2\omega) = -\frac{\varepsilon_0\kappa_p(2\omega)}{2}\left[\varepsilon'(\omega) + \frac{[\varepsilon'(\omega) + 2][\varepsilon'(\omega) - 1]}{3}\right] \quad (3)$$

$$d(\omega) = -\kappa_p(\omega)P_0\left[\frac{\varepsilon'(\omega_0) + 2}{3}\right] \quad (4)$$

where $\varepsilon'(\omega)$ is the real part of the dielectric constant at the ac modulation field frequency and $\varepsilon'(\omega_0)$ the dielectric constant at optical frequencies; κ_p is the frequency-dependent plate compliance.

If the real part of the dielectric constant ε' of the material is known, then it is possible to calculate the polarization P_0 from the ratio of the coefficients of the inverse-piezoelectric effect and the electrostriction. For most organic materials, $\varepsilon'(\omega_0)$ at optical frequencies is close to 2.5. Values for $\varepsilon'(\omega)$ of the PBLG film should be comparable to those reported for polymeric films at frequencies above the major dipole relaxation regime (*22*). For the data analysis values between 3 and 4 were chosen independent of frequency.

The value of P_0 as determined from the experimental data (Table 1) varies between 16 and 32 mC m^{-2}. The polarization decreases with increasing modulation frequency. This behavior is not yet understood, but it might indicate that the value for P_0 is affected by a tilting motion of the rodlike molecules or by a motion of the side chains. An estimate of the static polarization can be made on the basis of (*22*):

$$P_0 = \frac{N}{V}\mu\left[\frac{\varepsilon'(\omega_0) + 2}{3}\right] \quad (5)$$

assuming a perpendicular orientation of the rods; N/V is the number density of dipoles with dipole moment μ. Assuming a height of 1.5 Å and a dipole moment of 1.5 D per repeat unit as well as a surface area per polyglutamate chain of 195 $Å^2$ (*23*), the theoretically predicted polariza-

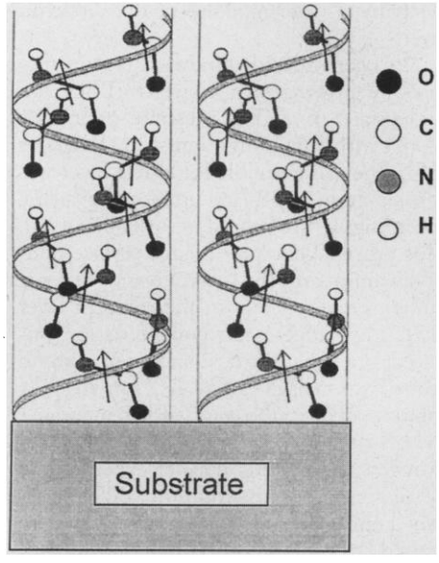

Fig. 1. Geometry of the "graft-from" film of a helical polyglutamate. Arrows indicate the directions of the individual dipole moments [polypeptide structure according to (*32*)].

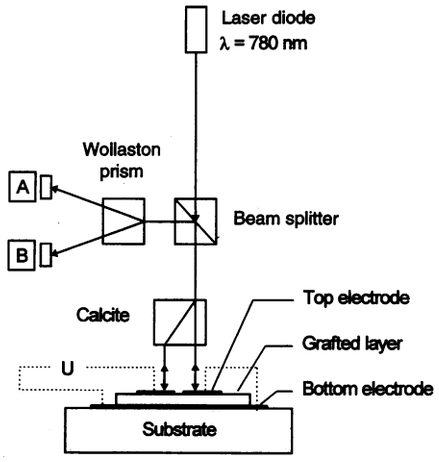

Fig. 2. Simplified scheme of the optical Nomarski interferometer (*13, 14*). The sample consists of a thin film sandwiched between a bottom electrode and two smaller top electrodes. At these electrodes two perpendicularly polarized beams are reflected. When voltage U is applied between only one of the top electrodes and the bottom electrode, the resulting change in film thickness causes a phase shift between the probe and reference beam. In the detection arm of the interferometer the recombined beam is split by a Wollaston prism into two beams with intensities A and B of perpendicular polarization and directed onto two photodiodes. At the working point of the interferometer, the difference of the two diode signals is proportional to the electric field–induced change in film thickness. The spot size of the laser beam reflected at the top electrode was ~1 mm.

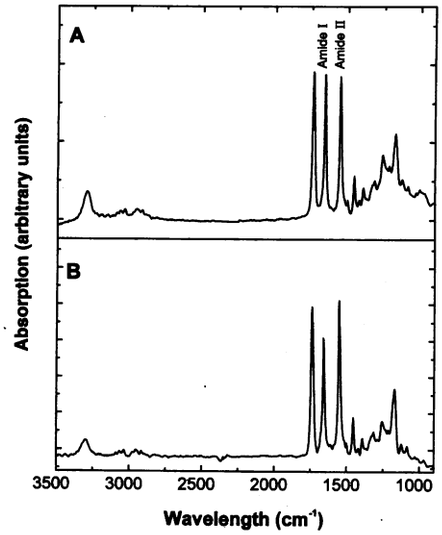

Fig. 3. Grazing-incidence IR absorption spectra of a grafted poly-γ-benzyl-L-glutamate layer on an aluminum-coated glass substrate (**A**) and of a LB film of 10 layers of PBLG on a gold-coated glass substrate (**B**).

tion is 26 mC m^{-2}. This estimate is very close to the average of the measured values for P_0. A more detailed interpretation would need to take into account the average tilt of the polymer chains relative to the surface normal.

A pseudo inverse-piezoelectric effect can also be measured in nonpolar materials in the presence of a dc offset field E_{bi} as, for example, caused by a built-in field across the sandwich layer. In this case, we must substitute for d in Eq. 2 an effective piezoelectric coefficient $d' = d + 2aE_{bi}$. We have measured the electromechanical properties of LB films of "hairy-rod" type polyglutamates (*24*) in a similar sandwich geometry between two aluminum electrodes. In these films the chains are exclusively oriented parallel to the substrate plane and the polarization is expected to be zero. For all LB films that we studied the piezoelectric (1ω) component was much smaller than the electrostriction (2ω) signal. This result demonstrates that the inverse-piezoelectric effect of the grafted films is caused by the large polarization in the film resulting from the polar alignment of the polymer chains.

The plate compliance of the grafted film can be evaluated from the electrostriction coefficient (Eq. 3). The plate modulus L (defined by the inverse of the plate compliance) varies between 37 and 47 GPa (Table 1), but there is no clear correlation with modulation frequency. These values are close to a Young's modulus of 34 GPa predicted for a single PBLG chain in a free-backbone simulation (*25*). In comparison, the determination of the elastic constants by Brillouin spectroscopy of "hairy-rod" type octadecyl$_{0.3}$-co-methyl$_{0.7}$-polyglutamate LB films yields a mechanical constant parallel to the rod of 10 GPa (*26*). Bulk values for the Young's modulus are even smaller (*27, 28*). Matrix effects as well as a more isotropic chain orientation are thought to account for these lower values.

Because the piezoelectric coefficient is proportional to the compressibility of the layer, the large mechanical modulus along the α-helical chain dampens the hope that ultrathin layers with huge piezoelectric coefficients can be built from polyglutamates. Even though the persistent polarization is large, comparable to values observed in ferroelectric polymers (*29*), the inverse-piezoelectric coefficient only reaches a level similar to that of quartz. Large piezoelectric and inverse-piezoelectric coefficients have been reported for materials such as $BaTiO_3$ (d = 190 pm V^{-1}), lead zirconate titanate (d = 289 pm V^{-1}), polyvinylidene fluoride (d = 28 pm V^{-1}) (*30*), and ferroelectric elastomers (d = 12.5 pm V^{-1}) (*31*). Despite the low inverse-piezoelectric coefficient of the grafted layer, the voltage sensitivity (defined as d/ε) is, however, quite comparable to that of commercially used piezoelectric materials. The advantage of the "grafting-from" concept is its feasibility for the growth of piezoelectric-active films directly on a variety of electrodes and even on flexible substrates, without the need for subsequent poling.

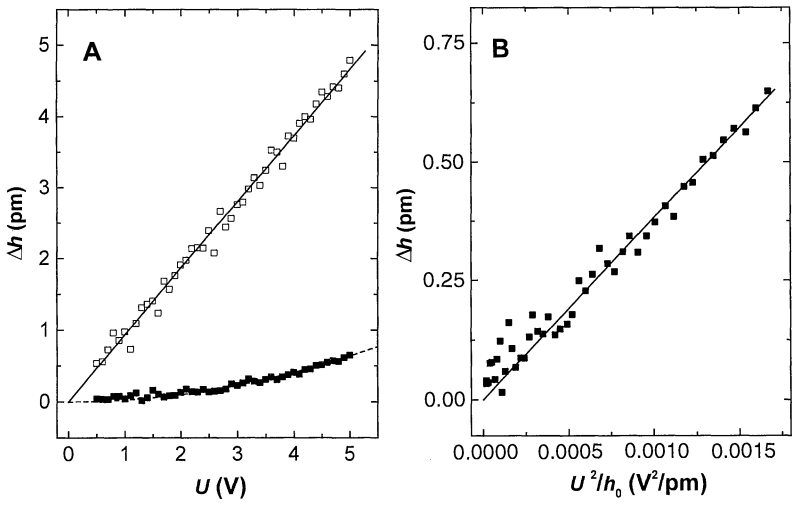

Fig. 4. Field-induced change in film thickness Δh due to the piezoelectricity (□) and electrostriction (■) of a grafted PBLG layer 15 nm thick. In the electrostriction experiment the frequency of the ac driving field was half the frequency used for the determination of the inverse piezoelectric coefficient (frequency = 1986 Hz). In (**A**) the field-induced modulation in thickness is plotted as a function of the amplitude U of the applied sinusoidal voltage. The slope of the linear fit to the piezoelectric date yields the inverse-piezoelectric coefficient d. In (**B**) the electrostriction data are plotted as a function of U^2/h_0. The linear regression yields the electrostriction coefficient a.

Table 1. Coefficients of the inverse-piezoelectric effect d and electrostriction coefficients a of a PBLG graft film 15 nm thick, measured at different frequencies of the field-induced change in film thickness (voltage range U = 0 to 3 V). We calculated the polarization P_0 and the plate modulus $L = \kappa_p^{-1}$ from these values for each frequency, using Eqs. 3 and 4. The indicated errors for P_0 and L correspond to the range of values taken for $\varepsilon'(\omega)$, which was varied between 3.0 (lower limits) and 4.0 (upper limits).

Frequency (Hz)	d (pm V^{-1})	a (pm^2 V^{-2})	P_0 (C m^{-2})	L (GPa)
156	1.323	984.6	0.032 ± 0.007	37 ± 8
1986	0.954	765.8	0.030 ± 0.007	47 ± 11
2500	0.912	943.3	0.023 ± 0.005	38 ± 8
5000	0.950	970.3	0.024 ± 0.005	37 ± 8
10000	0.793	916.2	0.021 ± 0.004	39 ± 9
20000	0.740	1089.2	0.016 ± 0.004	33 ± 7

REFERENCES AND NOTES

1. K. D. Singer, M. G. Kuzyk, J. E. Sohn, *J. Opt. Soc. Am. B* **4**, 968 (1987); D. M. Burland, R. D. Miller, C. A. Walsh, *Chem. Rev.* **94**, 31 (1994).
2. D. Lupo *et al.*, *J. Opt. Soc. Am. B* **5**, 300 (1988); J. P. Cresswell, G. H. Cross, D. Bloor, W. J. Feast, M. C. Petty, *Thin Solid Films* **210/211**, 216 (1992); R. Advincula, E. Aust, W. Meyer, W. Steffen, W. Knoll, *Polym. Adv. Technol.* **7**, 571 (1996).
3. D. Beyer, W. Paulus, M. Seitz, H. Ringsdorf, M. Eich, *Thin Solid Films* **271**, 73 (1995); W. B. Lin, W. P. Lin, T. J. Marks, *J. Am. Chem. Soc.* **118**, 8034 (1996); S. I. Stupp *et al.*, *Science* **276**, 384 (1997).
4. J. K. Whitesell and H. K. Chang, *Mol. Cryst. Liq. Cryst.* **240**, 251 (1994).
5. P. Palacios, P. Bussat, D. Bichon, *Angew. Makromol. Chem.* **193**, 77 (1991); K. Sano, S. Machida, H. Sasaki, M. Yoshiki, Y. Mori, *Chem. Lett.* **1992**, 1477 (1992); S. Machida, K. Sano, K. Sunohara, Y. Kawata, Y. Mori, *J. Chem. Soc. Chem. Commun.* **1992**, 1628 (1992); S. Machida, K. Sano, H. Sasaki, M. Yoshiki, Y. Mori, *ibid.*, p. 1626; T. L. Urano, S. Machida, K. Sano, *ibid.* **1994**, 231 (1994); S. Machida *et al.*, *Langmuir* **11**, 4838 (1995).
6. J. K. Whitesell and H. K. Chang, *Science* **261**, 73 (1993).
7. ———, C. S. Whitesell, *Angew. Chem.* **106**, 921 (1994).
8. M. L. C. M. Oosterling, E. Willems, A. J. Schouten, *Polymer* **36**, 4463 (1995).
9. R. H. Wieringa and A. J. Schouten, *Macromolecules* **29**, 3032 (1996).
10. A. Heise *et al.*, *Langmuir* **13**, 723 (1997).
11. B. F. Levine and C. G. Bethea, *J. Chem. Phys.* **65**, 1989 (1976).
12. H. Block and C. P. Shaw, *Polymer* **33**, 2459 (1992); P. G. Martin and S. I. Stupp, *ibid.* **28**, 897 (1987); Z. Tokarski *et al.*, *Chem. Mater.* **6**, 2063 (1994).
13. H.-J. Winkelhahn, H. H. Winter, D. Neher, *Appl. Phys. Lett.* **64**, 1347 (1994).
14. H.-J. Winkelhahn, T. Pakula, D. Neher, *Macromolecules* **29**, 6865 (1996).
15. We vapor-deposited the aluminum electrodes using a Balzer BAE 250 evaporation apparatus. The evaporation was performed through freshly polished and thoroughly cleaned brass masks with parallel slits 4 mm

wide. The thickness was chosen to be 72 nm. Details of the deposition procedure have been described elsewhere [G. Blum, F. Kremer, T. Jaworek, G. Wegner, *Adv. Mater.* **7**, 1017 (1996)].
16. I. Haller, *J. Am. Chem. Soc.* **100**, 8050 (1978).
17. Kurth and Bein have pointed out that the Haller silanization method results not in a monolayer film but rather in a film of two or three molecular layers due to cross-linking [F. G. Kurth and T. Bein, *Langmuir* **11**, 3061 (1995)]. We have analyzed the coupling layer on Si wafers and quartz slides by small angle x-ray reflection (SAXR) and have consistently found a thickness of 21 ± 3 Å, which agrees with the results of Kurth and Bein. The surface roughness was less than 6 Å.
18. R. H. Wieringa, E. A. Siesling, A. J. Schouten, in preparation.
19. Films of comparable thickness grafted on silicon had surface roughnesses of less than 1 nm as determined by SAXR.
20. Other reflection spectra of grafted PBLG films on various substrates will be published elsewhere. The present spectrum is typical for grafted PBLG films.
21. The equation used here was derived by F. Mopsik and M. G. Broadhurst [*J. Appl. Phys.* **46**, 4204 (1975)]. It is based on the Onsager approximation of the local field. We are aware of the recent discussion on this approximation [Y. Luo, H. Agren, K. V. Mikkelsen, *Chem. Phys. Lett.* **275**, 145 (1997)]. The polarization given here should, therefore, be treated as a crude estimate.
22. N. G. McCrum, B. E. Read, G. Williams, *Anelastic and Dielectric Effects in Polymeric Solids* (Dover, New York, 1967).
23. This estimate is based on the hexagonal packing of PBLG chains with an effective helix radius of 7.7 Å and thus represents a lower limit for the area. Oosterling has recently analyzed PBLG grafted from an aerosol [M. L. C. M. Oosterling, thesis, University of Groningen, Groningen Netherlands (1994)]. His data are consistent with a large area of 460 $Å^2$ per PBLG chain.
24. G. Duda *et al.*, *Thin Solid Films* **159**, 221 (1988).
25. J. Helfrich, R. Hentschke, U. Apel, *Macromolecules* **27**, 472 (1994).
26. F. Nizzoli *et al.*, *Phys. Rev. B* **40**, 3323 (1989).
27. E. Fukada, *Ultrasonics* (October 1968), p. 229; L. Jackson, M. T. Shaw, J. H. Aubert, *Polymer* **32**, 221 (1991).
28. H. Block, *Poly-(γ-Benzyl-L-Glutamate) and Other Glutamic Acid-Containing Polymers* (Gordan & Breach, New York, 1983).
29. T. Furukawa and J. X. Wen, *Jpn. J. Appl. Phys.* **23**, L677 (1984); J. Naciri, B. R. Ratna, S. Baral-Tosh, P. Keller, R. Shashidhar, *Macromolecules* **28**, 5274 (1995).
30. G. M. Sessler, in *Topics in Applied Physics*, G. M. Sessler, Ed. (Springer-Verlag, Berlin, 1987), p. 7.
31. T. Eckert and H. Finkelmann, *Macromol. Rapid Commun.* **17**, 767 (1996).
32. A. Wada, in *Polyamino Acids, Polypeptides, and Proteins*, M. A. Stahman, Ed. (Univ. of Wisconsin Press, Madison, 1962), p. 131.
33. We thank G. Glaßer for technical assistance with the Nomarski interferometer and M. L. C. M. Oosterling for fruitful discussions.

15 August 1997; accepted 3 November 1997

Coupling of South American and African Plate Motion and Plate Deformation

Paul G. Silver, Raymond M. Russo, Carolina Lithgow-Bertelloni*

Although the African Plate's northeastward absolute motion slowed abruptly 30 million years ago, the South Atlantic's spreading velocity has remained roughly constant over the past 80 million years, thus requiring a simultaneous westward acceleration of the South American Plate. This plate velocity correlation occurs because the two plates are coupled to general mantle circulation. The deceleration of the African Plate, due to its collision with the Eurasian Plate, diverts mantle flow westward, increasing the net basal driving torque and westward velocity of the South American Plate. One result of South America's higher plate velocity is the increased cordilleran activity along its western edge, beginning at about 30 million years ago.

The motions of tectonic plates are well-established components of plate tectonic theory. Yet, the manner in which plates interact, specifically how the forces driving adjacent plates are coupled to each other, is still uncertain. Plate interaction is most clear at a convergent margin. In a continent-continent collision, the leading edges of both plates are deformed and the velocities of both are constrained to be the same. Subduction represents a more subtle plate interaction, in which the overlying plate is deformed (producing marginal basins or cordilleran structures), although plate velocities are not obviously affected.

Our interest in plate interactions for Atlantic basin plates is motivated by the issue of cordillera formation along the western edge of the American plates, and its relation to the forces responsible for South American Plate (SA) motion. It was suggested (*1*, *2*) that Andean deformation is a result of the westward velocity of SA and the resistance to that motion by a more slowly retreating subducting Nazca slab. The velocity difference v between the trenchward velocity of the overlying plate and the natural retrograde velocity of the slab determines whether the back arc is under compression (positive) or tension (negative) [for example, (*3*)]. More generally, a temporal change in v should change the stress state of the back arc. In the case of SA, the onset of the latest phase of Andean deformation, beginning 25 to 30 million years ago (Ma) (*4*) was concurrent with an increase in the westward velocity of SA (*2*). A change in plate velocity must be due to a change in the force-balance on the plate. Thus, temporal variations in cordilleran deformation are an expected result of temporal changes in plate driving forces.

To examine this linkage, we analyzed the relative and absolute motion histories of the African Plate (Af) and SA over the last 80 million years (My) using fracture-zone orientations and sea-floor magnetic anomalies (*5*), and the motion of Af with respect to Atlantic basin hot spots Tristan da Cunha and St. Helena (*6*, *7*). The variations in SA and Af velocity vectors were determined from the stage poles of motion that were decomposed, as angular velocity vectors, into directions parallel and orthogonal to the relative plate motion direction (defined as the 80 My finite rotation pole). The corresponding plate directions are roughly east-west and north-south, respectively. While the half-spreading rate between the Af and SA remained relatively constant at 2 cm/year over the last 80 My, the absolute motion of Af slowed considerably beginning at about 30 Ma. Af's eastward velocity before this time averaged about 2.5 cm/year, but subsequently dropped to 1 cm/year (Fig. 1) (*8*). The combination of a roughly constant relative velocity and an abrupt reduction in Af's eastward velocity, requires a simultaneous increase in the absolute westward velocity of SA. During the last 30 My, this velocity increased from about 2.0 to 2.8 cm/year (Fig. 1). SA is currently moving faster relative to the hot spots than at any time in the last 80 My.

A simple explanation for the deceleration of Af is its collision with the Eurasian Plate (Eu), beginning about 38 Ma [for example, (*9*, *10*)], which is the largest and slowest moving plate (*11*, *12*). The simultaneous westward acceleration of SA, however, requires a separate mechanism. We propose that the change in SA's motion is the result of a flow-coupled plate interaction. If Af and SA are coupled to mantle flow (*13*), a change in Af motion perturbs the mantle flow field, which in turn alters the basal shear stress and, hence, the velocity of SA. The existence of this interaction is independent of whether the plates drive the flow or vice

P. G. Silver and C. Lithgow-Bertelloni, Department of Terrestrial Magnetism, Carnegie Institution of Washington, 5241 Broad Branch Road, N.W., Washington, DC 20015, USA.
R. M. Russo, Department of Geological Sciences, Northwestern University, Evanston, IL 60208, USA.

*Present address: Department of Geological Sciences, University of Michigan, Ann Arbor, MI, 48109, USA.